

We are IntechOpen, the world's leading publisher of Open Access books Built by scientists, for scientists

6,900

Open access books available

186,000

International authors and editors

200M

Downloads

Our authors are among the

154

Countries delivered to

TOP 1%

most cited scientists

12.2%

Contributors from top 500 universities



WEB OF SCIENCE™

Selection of our books indexed in the Book Citation Index
in Web of Science™ Core Collection (BKCI)

Interested in publishing with us?
Contact book.department@intechopen.com

Numbers displayed above are based on latest data collected.
For more information visit www.intechopen.com



Systematics in WMAP and Other CMB Missions

Hao Liu¹ and Ti-Pei Li²

¹Key Laboratory of Particle Astrophysics, Institute of High Energy Physics, Chinese Academy of Sciences

²Department of Physics and Center for Astrophysics, Tsinghua University, Key Laboratory of Particle Astrophysics, Institute of High Energy Physics, Chinese Academy of Sciences China

1. Introduction

1.1 The success of WMAP

When the WMAP team released their unprecedentedly precise CMB anisotropy maps in the year of 2003 (Fig. 1, Bennett et al. (2003)), everyone were celebrating the finally arrival of experimental foundation of precision cosmology. It did worth all praises, because the measured CMB power spectrum was so beautifully consistent with the theoretical expectation, and a clear scene of the birth and growth of a flat and ordered Universe seems to be right within the reach of our hands, as well as the first precision percentage estimation of its contents. Many people begin to believe that, we no longer need to be bored by one new cosmic model per day, and the Big Bang scene and Λ CDM model will be good enough to give us satisfactory explanation to anything we want to know.

It's not strange that there still remains some small disharmonious flaws, like an unexpectedly low quadrupole power (Bennett et al., 2003; Hinshaw et al., 2003b), alignment issues and NS asymmetry (Bielewicz et al., 2004; Copi et al., 2007; Eriksen et al., 2005; 2007; Hansen et al., 2004; 2006; Wiaux et al., 2006), non-Gaussianity including cold/hot spots (Copi et al., 2004; Cruz et al., 2005; 2007; Komatsu et al., 2003; Liu & Zhang, 2005; McEwen et al., 2006; Vielva et al., 2004; 2007), etc. Among all these flaws, the loss of the quadrupole power is the

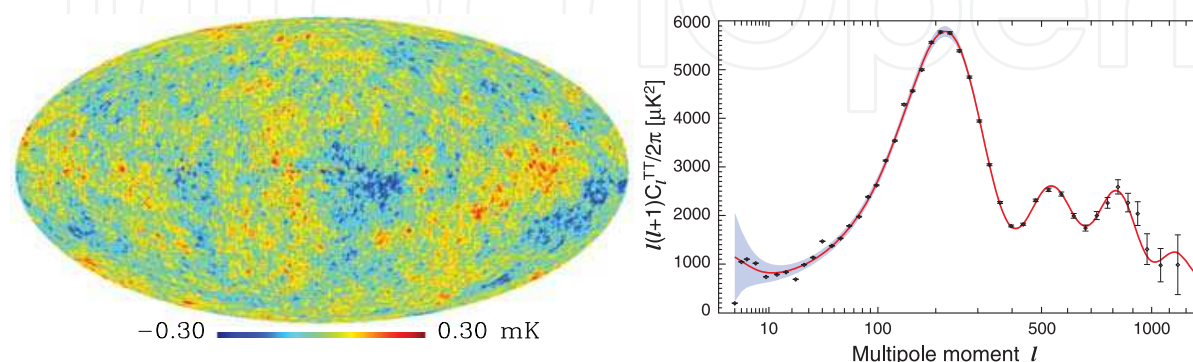


Fig. 1. The CMB anisotropy map and power spectrum obtained by WMAP (Bennett et al., 2003).

sharpest one: We can see clearly from the right panel of Fig. 1 that the first black dot starting from the left (which represents the measured CMB quadrupole power) is much lower than theoretical expectation (the red line). However, in several years, these flaws or doubts don't really shake the success of WMAP, partly because they have a general difficulty: it's hard to distinguish the exact cause of these phenomenons, whether it's just something occasional, or due to a cosmic issue, or due to a measurement error. Given different answer to the cause, the corresponding treatment would be significantly different: For something occasional, nothing need to be done, and a cosmic issue need only to be solved in the frame of cosmic theories, but for a measurement error, it must be corrected by improving the measurement or data processing before considering any further theoretical efforts. Although, in several years, there are no strong evidences for us to find out the true cause, the cosmic issue is apparently preferred, because it's really difficult for a researcher outside the WMAP team to deal with the mission details. Especially, almost nobody really believes that the WMAP team, as such a large, experienced and professional group, could make a significant mistake in such an important experiment. Therefore, unless there appears something more evidently suggesting a potential measurement error, the effort of rechecking the WMAP detecting and data processing system will probably never be seriously considered, and the WMAP cosmology will never be questioned from the technical side.

1.2 Two early discovered anomalies

We had found such evidences between 2008 and 2009 (Li et al., 2009; Liu & Li, 2009a), and these findings had directly driven us to explore the WMAP raw data to find the reason for them. It's interesting that, till now we haven't found explanations that are satisfactory enough for the two early discovered anomalies, but instead, we have found anomalies that seem to be much more important than them.

1.2.1 The pixel-ring coupling issue

The first anomaly is related to a pixel-ring coupling issue on the CMB maps. To understand this, we need to know a few things about the way that the WMAP spacecraft measures the anisotropy of the CMB. The CMB anisotropy is extremely weak: about 10^{-5} of the well known nearly symmetric 2.73 K blackbody CMB emission. To detect such a weak signal, they have found a nice way to enhance the anisotropy relatively: The spacecraft receives CMB signals coming from two different directions by two highly symmetric antennas, and records only the difference between them to cancel the uniform 2.73 K blackbody CMB emission. This also help to counteract some of the systematical effects that affects the two antennas in the same way. In such an observational design, the separation angle between the two antennas is an important factor, which is 141° in the WMAP mission. It's apparently important to ensure that, when the measured differential signal is transformed into full-sky anisotropy maps by a sophisticated map-making process, the 141° separation angle, as an artificial thing, leaves completely no trace on the final map. In other words, there should be no clue for us to "guess" the man-made 141° separation angle from the final natural CMB map.

Intuitively, we would feel that, when the two antennas point at pixel A with a small deviation to 2.73 K (either higher or lower) and pixel B with very high temperature above 2.73 K respectively, the recorded differential data will have a large value; however, since we actually don't know either A or B temperature a priori, we will have at least two equally reasonable guesses: A is very cold or B is very hot. If the map-making from differential data is reliable,

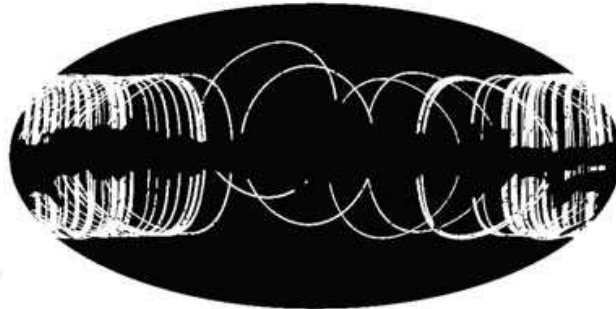


Fig. 2. The 141° scan rings of 2000 hottest pixels on the CMB sky.

then we would be able to deduce which is true with more observations that involves more pixels; however, if something doesn't work well, then we may obtain a wrong guess for A is very cold, or maybe not that bad: A is just slightly colder than what is expected. If such an deviation does exist, then it can be detected by checking the average temperature of all pixels in a ring that is 141° away from the very hot pixel B. This is right what we have done in Liu & Li (2009a).

In that work, we pick out 2000 hottest pixels from the CMB anisotropy map provided by the WMAP team, and select all pixels on the corresponding 141° rings which look like Fig. 2. The average temperature of these pixels are calculated for all WMAP bands Q, V and W, which are between $-11 \mu\text{K}$ and $-13 \mu\text{K}$, and these values are $2.5 \sim 2.7\sigma$ lower than expectation.

This is not enough yet: Although the values are really colder than expected, it can still be something occasional. However, the problem will become more serious if such a phenomena appear to be stuck on 141° , the man-made physical separation angle between the two antennas. It's possible to test this: Suppose that the final CMB map is perfect, then it must be completely "blind" to the physical separation angle, thus we can set a "guessed" value for the separation angle, then pick out each center pixel and the average temperature on the corresponding ring as a pair, and calculate the correlation coefficients between them to see if the 141° separation angle has an outstanding correlation strength. This is found to be true: By force the angular radius of the scan ring to change between 90° to 160° , we discovered that the anti-correlation strength is really strongest around 141° . Moreover, if the choice of center pixel is limited outside the foreground mask (so that the center pixel temperatures will not be very hot), then the correlation will be significantly weaker, indicating that these center pixels are less likely to arouse a cold ring effect (Fig. 3). With these self-consistent evidences, it's apparently more reasonable to deduce that the pixel-ring coupling is some kind of a systematical error, not something cosmic or occasional.

1.2.2 The T - N correlation issue

Another anomaly is much easier to understand: In any physical experiment, the most often adopted way to increase the accuracy and to suppress the noise is to apply more observations. With increasing number of observation, the result should be closer and closer to the true value, and converge at a accuracy level of $1/\sqrt{N_{obs}}$, but it's never expected that the result should subsequently increase or decrease with N_{obs} . In other words, there should be no correlation between the number of observation and the derived values. If this is seen with

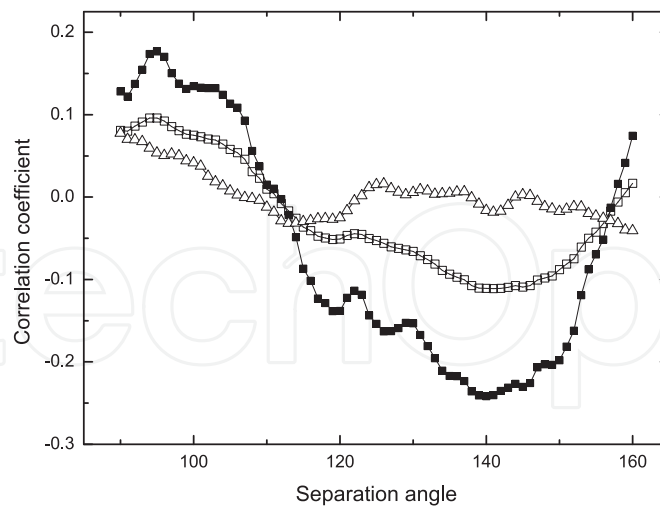


Fig. 3. The dependence of the correlation coefficients upon the separation angle. *Solid square*: The center pixels are limited within the hottest pixels on the CMB sky. *Empty square*: The center pixels being all pixel on the CMB sky. *Triangle*: The center pixels are limited outside the foreground mask.

enough significance, then it's almost certainly that a problem will exist in the measurement system, because the number of observation has nothing to do with the theoretical issues.

We did see this in the WMAP data (Li et al., 2009): the average absolute magnitude of the correlation coefficients between the WMAP CMB anisotropy temperatures and corresponding N_{obs} are $4.2\sigma \sim 4.8\sigma$ higher than expectation, and their distribution also significantly deviates from expected Gaussian distribution (Fig. 4), indicating that there is very likely a systematical problem in the WMAP mission, which has remarkably contaminated the final CMB anisotropy result.

When we see the river is muddy and believe it should not be like this, we will certainly go upstream to see where comes the mud. These two anomalies give rise to a doubt on the WMAP data, and will certainly drive us upstream for the origin, although the way is really cliffy.

2. Reprocessing the raw data

It's a tedious story how we explored the raw data and saw many false "differences" to the WMAP team. In brief, for many times when we worked on the WMAP raw data, we had seen this or that kind of "little surprises" smashed quickly by following tests, that we nearly despaired of finding anything worth noticing. This illustrated from another side how excellently had the WMAP team done. But at last we saw something that was not negligible on the problem of the CMB quadrupole. It's funny that it also started with a mistake: we actually got a much higher quadrupole value than WMAP at first, which was certainly welcome by theorist, but like usual, in a few days we found this is just another mistake. However, the turning point came silently before we realized it: When we corrected the mistake, the CMB quadrupole didn't come back and disappeared almost completely. We thought this was just one more fragile "little surprise", but we were wrong again.

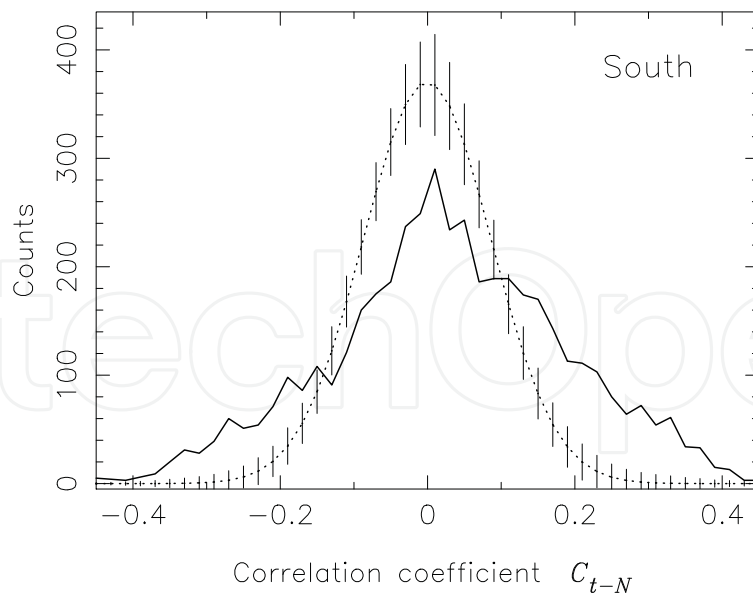


Fig. 4. The distribution of the T-N correlation coefficients (*solid*) compared with expectation and corresponding error bar given by 50,000 simulation (*dash*). It's very easy to see the deviation of real data from expectation.

2.1 Some basic thing about the map-making

In producing output full sky CMB temperature maps from the raw time-order differential data (TOD), the WMAP team have provided a beautiful formula (Hinshaw et al., 2003a): Let the CMB temperature anisotropy be a single-column matrix \mathbf{T} with N_{pix} rows (for N_{pix} pixels on the sky), and the observation course be represented by a matrix \mathbf{A} with N rows, N_{pix} columns (N is the total number of observations, which is much higher than N_{pix}) that is mostly zero, except for one 1 and one -1 in each row, then the TOD \mathbf{D} can be described by a matrix multiplication:

$$\mathbf{A}\mathbf{T} = \mathbf{D} \quad (1)$$

The j th line of Equation 1 is actually a simple sub-equation:

$$T_j^A - T_j^B = D_j, \quad (2)$$

where A and B stand for the two antennas, and $j = 1, \dots, N$. The difficulty in solving for the CMB temperatures \mathbf{T} is that \mathbf{A} is not a square matrix. In linear algebra, this means either Equation 1 has no solution, or it contains many redundant rows, because N is much higher than N_{pix} . However, we can multiply the transpose of \mathbf{A} to both side and obtain a square matrix $\mathbf{A}^T\mathbf{A}$:

$$(\mathbf{A}^T\mathbf{A})\mathbf{T} = \mathbf{A}^T\mathbf{D} \quad (3)$$

Then the solution can be formally obtained by:

$$\mathbf{T} = (\mathbf{A}^T\mathbf{A})^{-1}\mathbf{A}^T\mathbf{D} \quad (4)$$

Equation 4 seems to be simple and beautiful, but it's incorrect in linear algebra, because $\mathbf{A}^T\mathbf{A}$ is a singular matrix and $(\mathbf{A}^T\mathbf{A})^{-1}$ doesn't exist. Actually, even if $(\mathbf{A}^T\mathbf{A})^{-1}$ exists, there is no way to exactly solve for such a huge matrix with millions of rows and columns. An approximation

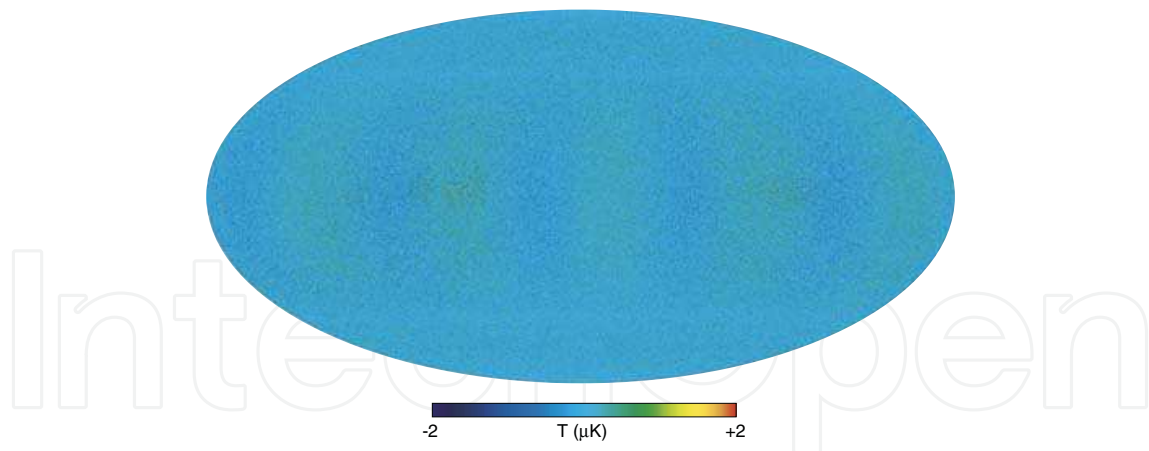


Fig. 5. The expected residual map-making error from Fig. 2 of Hinshaw et al. (2003a), which is negligible, and can be even reduced by more iterations. However, the observation noise is not taken into account here.

for $(\mathbf{A}^T \mathbf{A})^{-1}$ is a $N_{pix} \times N_{pix}$ diagonal matrix¹:

$$\mathbf{N}^{-1} = \begin{pmatrix} 1/N_1 & 0 & \cdots \\ 0 & 1/N_2 & \cdots \\ \cdots & \cdots & \cdots \end{pmatrix}, \quad (5)$$

where N_i is the total number of observation for the i th map pixel, $i = 1, \dots, N_{pix}$ and $\sum_i N_i = N$. Based on this approximation, an iterative solution can be performed to estimate the final CMB temperatures \mathbf{T} .

The iterative solution is simple: we give an initial all-zero guess \mathbf{T}^0 to the CMB anisotropy map \mathbf{T} , and, based on that, use the TOD \mathbf{D} to improve the guess by $T_j^{1,i_A} = T_j^{0,i_B} + D_j$ or $T_j^{1,i_B} = T_j^{0,i_A} - D_j$ (see also Equation 2), where T_j means the j th temperature estimation corresponding to the j th observation, and i_A stands for the A-side pixel in this observation, so do i_B . In this way, each D_j gives two improved estimations T_j^{1,i_A} and T_j^{1,i_B} for the positive/negative sides one the map respectively. The improved \mathbf{T}^1 is the assembly of all T_j , averaged at each sky pixel i respectively: $T_i^1 = (\sum_j T_j^{1,i_A=i} + \sum_j T_j^{1,i_B=i})/N_i$ (T_i mean the averaged temperature of the i th pixel on the sky), and the final CMB anisotropy map is produced by 50 to 80 iterations like this².

Although a strict solution to \mathbf{T} is impossible, the iterative solution works quite well, at least according to simulation: As presented by the WMAP team (Fig. 5), discarding the observation noise and the uncertain monopole, the residual full sky map-making error is negligible. This has been confirmed by us, but we have found that for such an excellent convergence in Fig. 5, the average of odd and even iteration rounds should be used, which was not mentioned in the WMAP documents.

¹ Since $(\mathbf{A}^T \mathbf{A})^{-1}$ doesn't exist, "approximation for $(\mathbf{A}^T \mathbf{A})^{-1}$ " means this matrix multiplies $\mathbf{A}^T \mathbf{A}$ gives an output matrix that is almost unitary.

² The map-making processes described here are simplified for ideally symmetric antennas with perfectly stable responses. For equations including necessary fine corrections, please refer to Hinshaw et al. (2003a)

2.2 Be consistent to WMAP first

Although our emphasis is the difference to the WMAP team, we would like to illustrate at the very beginning that we are now able to obtain fully consistent results to the WMAP team using our own map-making software, as shown in Fig 6. The reason is: Unless we are able to do so, the crucial reason of the **difference** between our results and WMAP will never be determined, because we will be lost in countless technical details, each seems to be able to cause some specious "differences" in this or that way, as briefly but incompletely listed below:

- f^{-1} noise (an equipment feature)
- Usage of the processing mask (determines how many raw data are unused)
- TOD flag issue (likewise)
- Antenna imbalance (the antennas are not absolutely symmetric)
- Problem in resolving the spacecraft velocity (affects the Doppler signal and calibration)
- The Sun velocity uncertainty (likewise)
- Dipole signal subtraction (remove the unwanted Doppler signal)
- Foreground subtraction (remove the unwanted foreground emission)
- Incomplete sky coverage (some sky regions are unused in calculating the CMB power spectrum)
- Beam function correction (which can greatly suppress the small scale anisotropy)
- Window function correction (likewise)
- Map making convergence (does the iteration converges well?)
- The antenna pointing vectors (affected by various factors)
- ...

Needless to say, nothing valuable can be obtained before we climb out of such a bottomless list. However, once we get Fig. 6, we will then be able to clearly identify which item in this list makes the major contribution to the difference between WMAP and us. This can be done by changing one item one time, and see how it takes effect on the final CMB maps and power spectrum.

3. The origin of the difference between our results and WMAP

In time sequence, the difference in the CMB anisotropy maps and power spectrum is discovered first, and then the origin of the difference is found and confirmed as illustrated in Section 2.2. This is not the end of the problem, because we need to check whether WMAP or us is more likely to be correct. Soon after that, several evidences supporting our results are obtained, and we also found reasonable explanations to why WMAP could be wrong. Such explanations is not only valuable in improving the WMAP result, but also valuable in preventing future CMB detecting mission from making the same mistake. We will follow this sequence, and present our work step by step.

3.1 The difference in the CMB result using the same raw data

After tottering through the raw data processing, we finally get a tentative CMB result in the end of 2008 (Liu & Li, 2009b), which looks very similar to the WMAP official release, as shown in Fig. 7 However, if we subtract our map from WMAP and smooth the result, the difference can be clearly seen, which is a four-spot structure, two hot and two cold. This is a typical quadrupole structure. More interestingly, such a difference is almost the same to the claimed

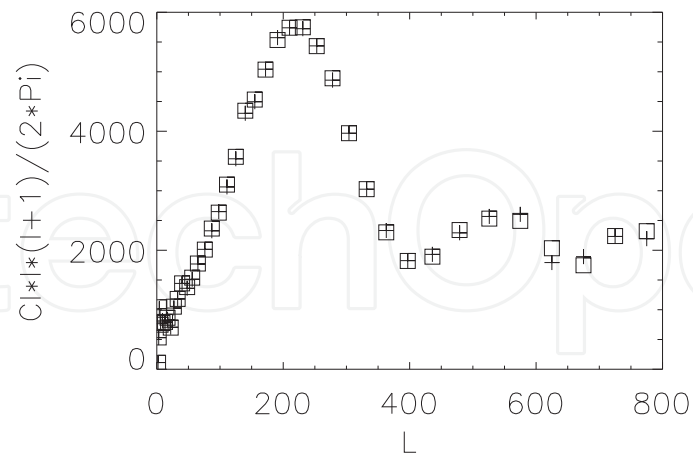


Fig. 6. We are now able to obtain fully consistent CMB result to the WMAP team using our own software but adopting their convention. This greatly simplify the search for the origin of the difference. *Square*: CMB power spectrum obtained from the WMAP official maps. *Cross*: CMB power spectrum obtained from our maps using their conventions.

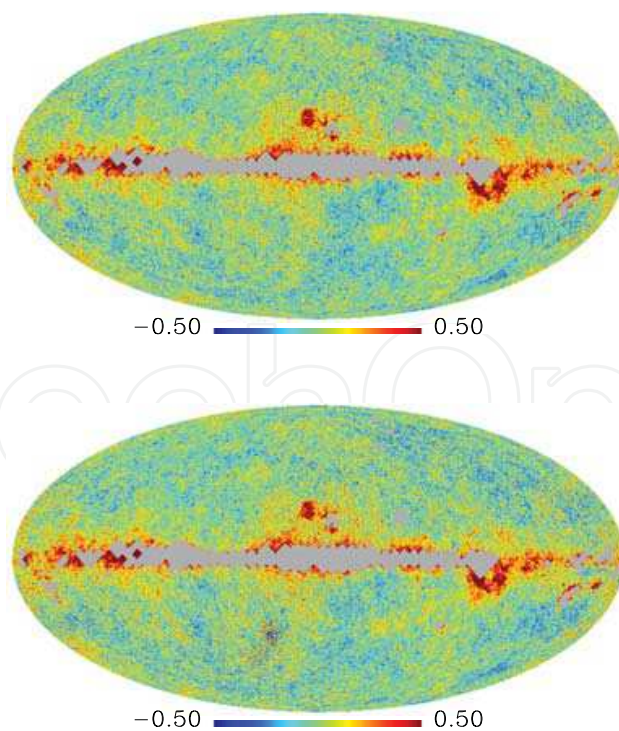


Fig. 7. The Q1-band CMB temperature maps by the WMAP team (*left panel*) and by us (*right panel*). Both in the Galactic coordinate and the unit is mK. They look almost the same.

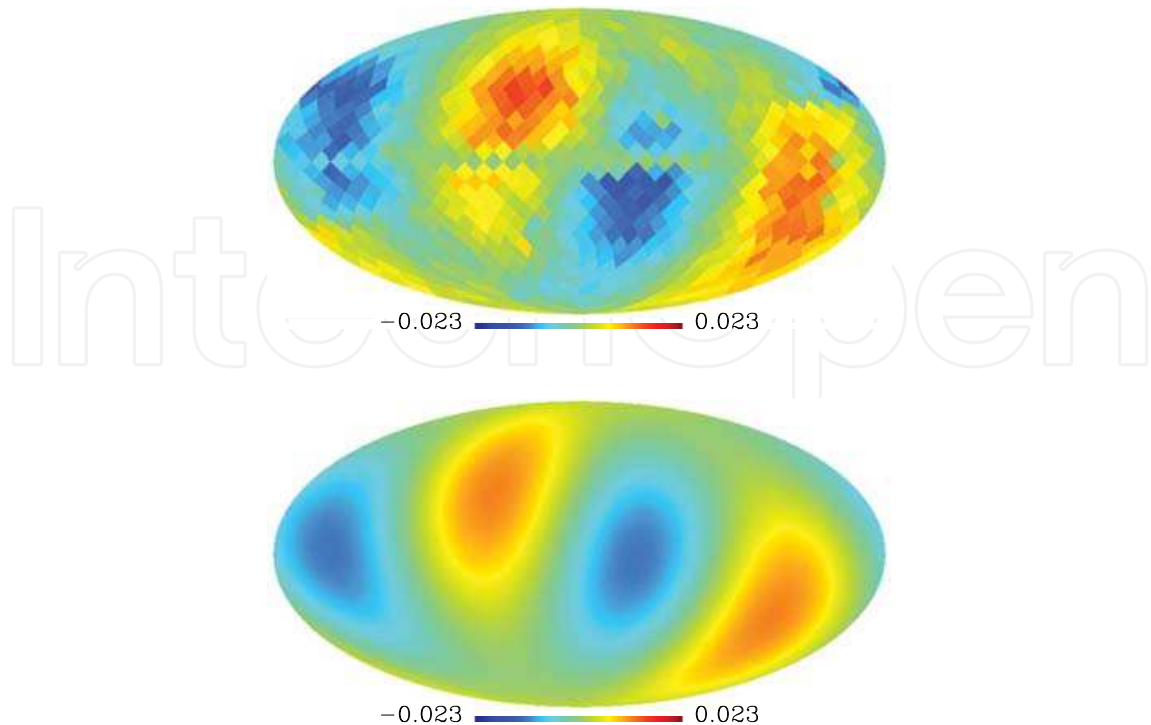


Fig. 8. This figure is to show the large-scale CMB structure difference between WMAP and us. *Left panel:* The CMB map of WMAP minus ours, smoothed to $N_{side} = 8$, so that it's dominated by large-scale differences. *Right panel:* The quadrupole component of the released WMAP CMB anisotropy map. They are amazingly similar, which casts doubt on the WMAP data.

CMB quadrupole structure by WMAP (Fig. 8). This phenomena certainly worths further consideration.

The CMB power spectrum is calculated by spherical harmonic decomposition. The spherical harmonics $Y_{lm}(\theta, \phi)$ are known as a family of normalized, orthogonal and complete functions on the sphere, which is widely used to analyze problems on the sphere including the CMB anisotropy. The spherical harmonic coefficients are calculated by:

$$\alpha_{lm} = \int T(\theta, \phi) Y_{lm}^*(\theta, \phi) \sin(\theta) d\theta d\phi, \quad (6)$$

and the CMB power spectrum is obtained by:

$$C_l = \frac{1}{2l+1} \sum_{m=-l}^l |\alpha_{lm}|^2 \quad (7)$$

Besides Equation 7, there are many further corrections in calculating the final CMB power spectrum; however, as illustrated in Section 2.2, we can confirm that we have appropriately applied all these corrections by the consistency between the crosses/squares in Fig. 6 (so we see how important it is to be consistent to WMAP first). Based on the confirmed consistency, we can conclude that the differences in both large and small scale power spectra (Fig. 9) are

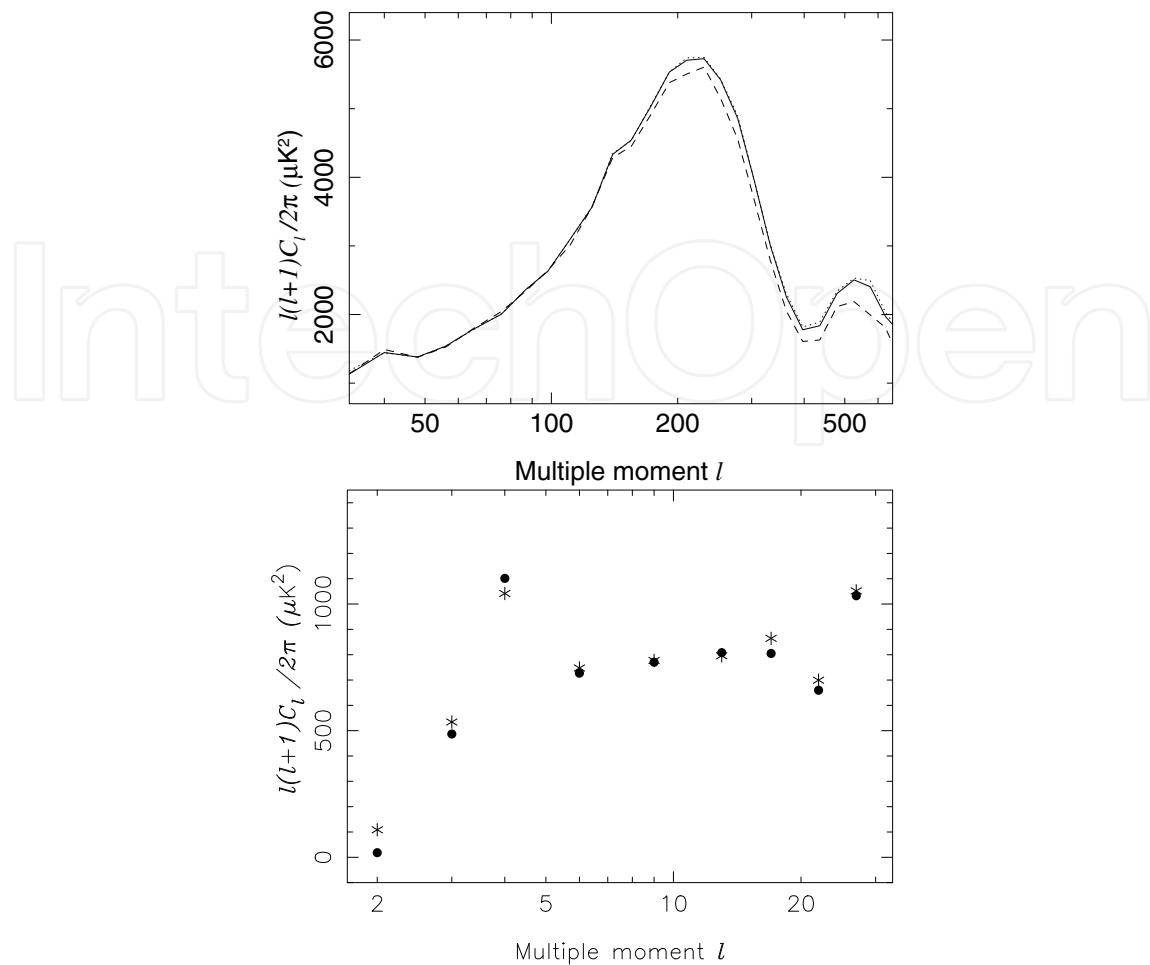


Fig. 9. *Left Panel:* The CMB power spectra derived with our software from our new map (*dash line*), with our software but from the WMAP official maps (*dotted line*), and directly released by the WMAP team (*solid line*). By the difference between the solid line and dash line, we can see that the small scale CMB power spectra derived by us and WMAP are apparently different. *Right Panel:* The large scale CMB power spectra by us (*dot*) and by WMAP (*asterisk*). We can see that only the quadrupole is significantly different.

not due to the power spectra estimation, but due to a possible issue in the map-making from the raw data.

3.2 The origin of the difference

We took a long time to search for the origin of the differences. Finally we found that it's due to an antenna pointing vector issue. This had been noticed by us before, but was ignored at first because it's really too small.

The WMAP spacecraft doesn't record the antenna pointing vector for each observation: The pointing vectors are much less frequently recorded than the science data in order to reduce the data file size. Therefore in raw data processing, we need to interpolate the available antenna pointing vector to calculate the unrecorded pointing vectors for each observation. In our data processing program, one of the interpolation parameters is slightly different to WMAP, which

causes the calculated pointing vectors to be different for about half a pixel to them. This looks really a trivial thing, but it's right the key of all differences shown in Fig. 8 and 9.

4. Zigzag

In most cases, when you find the origin of the problem, the case will soon be totally solved. However, for us, discovering the antenna pointing vector issue is just the beginning of the zigzag pursuit.

4.1 WMAP seem to be right?

When we study the key of the difference: the interpolation parameter change carefully, we feel that WMAP is probably correct, because they have used the center of each observation interval as the effective antenna pointing vector for that observation, but we have used the start of it. Since WMAP is continuously receiving the microwave signal, the center of the observation is apparently a better choice. Thus the prospect of our finding seem to be dim at first.

4.2 A doubtful point: evidence against WMAP

However, an unconvinced fact still remain in our mind: When adopting our interpolating settings, nearly 90% of the CMB quadrupole (the component with $l = 2$) will disappear. If this doesn't look suspicious enough, then from another point of view we will see what it actually means.

The antenna pointing vector difference affects the CMB quadrupole via the Doppler signal subtraction. In the WMAP observation, the strongest contamination to the CMB signal is the Doppler signal caused by the motion of the spacecraft towards the CMB rest frame. This particular signal can be calculated by:

$$d = \frac{T_0}{c} \mathbf{V} \cdot (\mathbf{n}_A - \mathbf{n}_B), \quad (8)$$

where T_0 is the 2.73 K CMB monopole, c is the speed of light in vacuum, \mathbf{V} is the velocity of the spacecraft relative to the CMB rest frame, and \mathbf{n}_A , \mathbf{n}_B are the antenna pointing vectors. We can see clearly that, if the antenna pointing vectors are slightly different, either on \mathbf{n}_A or \mathbf{n}_B or both, then the calculated Doppler dipole signal d will be consequently different:

$$\Delta d = \frac{T_0}{c} \mathbf{V} \cdot \Delta \mathbf{n}, \quad \Delta \mathbf{n} = \Delta \mathbf{n}_A - \Delta \mathbf{n}_B. \quad (9)$$

It's interesting that, from Equation 9 we can see that we don't have to know any CMB information in calculating Δd . Therefore, the deviation upon the CMB quadrupole caused by possible antenna pointing vector error (no matter what reason) can be calculated independently of the CMB maps or CMB detection. This has been done by us (Liu, Xiong & Li 2010), and the result is again almost same to the released WMAP CMB quadrupole, as shown in Fig. 10. Now we can see the real puzzle: The "CMB" quadrupole has been reproduced without any observation, which is absurd. Theoretically speaking, this is not impossible, but a much more reasonable explanation is that the claimed "CMB" quadrupole is actually a systematical error.

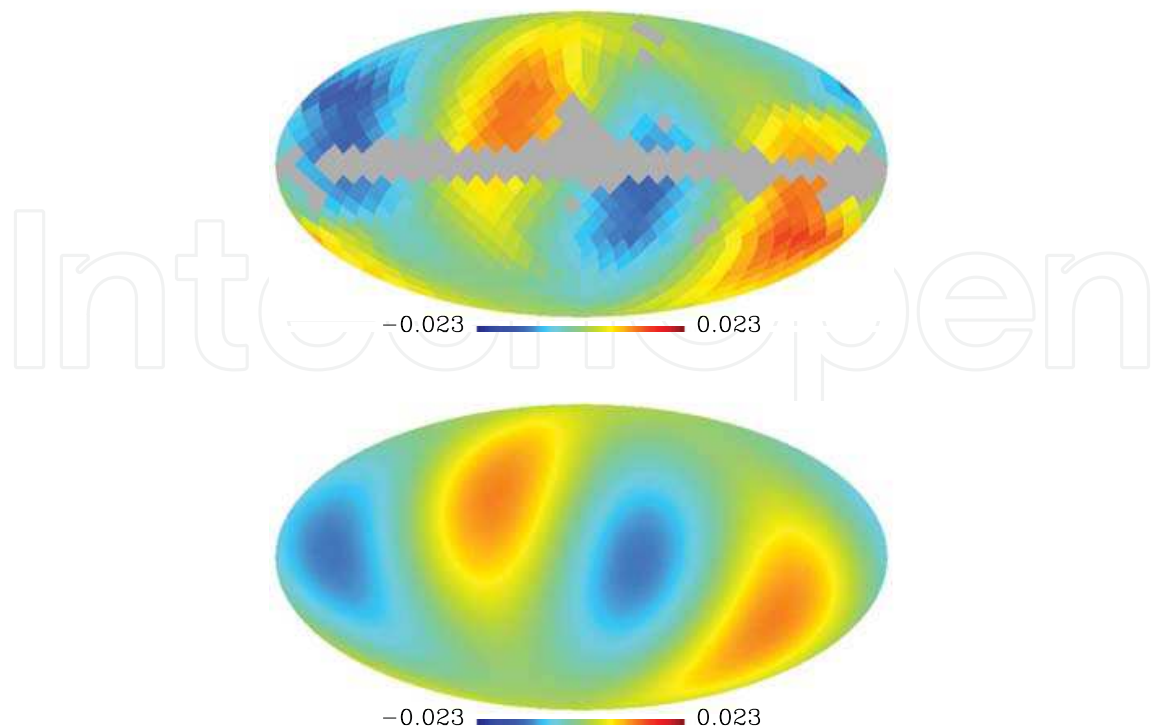


Fig. 10. *Left Panel:* The expected deviation on final CMB temperature map caused by Δd (see Equation 9). Note that there is no inclusion of any CMB signal in obtaining this figure. *Right Panel:* The claimed CMB quadrupole by WMAP.

The results in Fig. 10 has been independently reproduced by Moss et al. (2010) and Roukema (2010a), and has been regarded as an important evidence in questioning the WMAP cosmology (Sawangwit & Shanks, 2010). The software used to obtain this result is the same software written by us for re-processing the WMAP TOD, which is publicly available on the websites of the cosmocoffee forum³ or the Tsinghua Center for Astrophysics⁴.

4.3 WMAP is supported again?

Since the focus of the problems seem to be upon the antenna pointing vectors, a third party test on this is soon applied by Roukema (2010a), in which he believe that, if there is an antenna pointing vector error, then the generated CMB maps will be blurred, thus by checking the image sharpness of the CMB maps, we can decide whether there really exists such an error. His conclusion is that, the WMAP official maps are apparently less affected by the blurring effect compared to ours. This is a strong supporting evidence for WMAP being correct, and the prospect of our finding seems to be dim again.

4.4 Not the end: more details discovered

In fact, even in Roukema (2010a), the author didn't conclude that there will surely be no problem in the pointing vectors. He pointed out that the antenna pointing vector issue might

³ <http://cosmocoffee.info/viewtopic.php?t=1541>

⁴ http://dpc.aire.org.cn/data/wmap/09072731/release_v1/source_code/v1/

still take effect in the data calibration. Although such an possibility seems to be minor, it was soon confirmed by following works by him and us.

Three months later after Roukema's previous work, by checking the median per map of the temperature fluctuation variance per pixel, he discovered that, in a very high significance level, there does seem to be an antenna pointing vector error in the raw data, possibly due to the data calibration (Roukema, 2010b). We have confirmed this finding with different method (Liu, Xiong & Li, 2011), and the obtained results are very well consistent to Roukema (2010b). This seems to be puzzling: How can the same problem, the antenna pointing issue, be confirmed and rejected at the same time?

4.5 Real and equivalent pointing vector errors

To answer this question, we need to have a look at the antenna pointing issues again. The antenna directions are affected by at least three independent factors:

- *Direct pointing error (e.g., the antennas are misplaced).*
- *Timing error*
- *Sidelobe uncertainty*

All these three effects can cause antenna pointing vector errors; however, we have confirmed that the 1st and 2nd effects can further cause both the blurring effect and power spectrum deviation, and the 3rd causes only the power spectrum deviation. Thus the evidences found in Roukema (2010a) doesn't in principle conflict with Roukema (2010b) and Liu, Xiong & Li (2011). Moreover, all these three articles have also pointed out that the antenna pointing error can possibly take effect in the calibration stage without blurring the final image, which lead to the same conclusion.

Now we have a clear logical sequence: The three reasons listed above (possibly more) cause antenna pointing vector errors (real or equivalent), and the antenna pointing vector errors further cause all the CMB deviations discussed in this article. The antenna pointing vector error is hence the node of the entire problem.

4.5.1 Real pointing vector error

It's easy to understand the first factor, thus we introduce no more discussion for it. The second factor is due to the rotation of the spacecraft: In order to scan the sky, the spacecraft must rotate continuously, thus we must know the angular velocity and the local time to calculate the antenna pointing vectors. If there is a timing error, then the derived antenna pointing vectors will certainly be mistaken. In Liu, Xiong & Li (2010), we have discovered that the WMAP spacecraft attitude data are asynchronous to the CMB differential data, thus existence of the timing error is apparently possible. This is further confirmed in Liu, Xiong & Li (2011) and Roukema (2010b).

Both the first and the second factors are called real pointing vector errors, because the antenna pointing vectors will be substantially in error due to them. However, besides the real pointing vector error, there is also equivalent pointing vector error caused by the third factor. In this case, the antenna pointing vectors might be accurate, but the recorded data are twisted, as if there were a pointing vector error.

4.5.2 Equivalent pointing vector error

The third factor is a hidden factor that has never been noticed before. Generally speaking, radio antenna has response to all 4π solid angle, not merely along its optical pointing. For the WMAP antennas, the 4π response is described by a normalized gain G : If there is only one beam b coming from a direction marked by pixel i , then the recorded signal should be $S = G_i b$. For full sky signal like the CMB, the recorded signal is⁵:

$$S = \frac{1}{N_{pix}} \sum_{i=0}^{N_{pix}-1} G_i T_i. \quad (10)$$

Since WMAP works in differential mode, the equation for WMAP should be:

$$D = \frac{1}{N_{pix}} \sum_{i=0}^{N_{pix}-1} (G_i^A - G_i^B) T_i, \quad (11)$$

where N_{pix} is the number of pixels on the sky, G_i^A and G_i^B are the normalized gains for the A-side and B-side antennas in the spacecraft coordinate⁶ respectively, T_i is the CMB temperature. According to the WMAP convention, the normalization rule is $\sum_{i=0}^{N_{pix}-1} G_i = N_{pix}$.

In Equation 11, only a few pixels stands for the main lobe, and most pixels belong to the sidelobe, but the sidelobe pixels have much lower gain amplitudes: the summation of all sidelobe normalized gains are less than 5%. The standard method to clean the sidelobe contamination is by deconvolution; however, this is very complex and slow, and the biggest disadvantage is missing of a clear physical picture. We discovered that the deconvolution can be greatly simplified for some special full sky signals, and we can get a very clear and simple physical scene for them. Fortunately, the strongest contamination in CMB experiments, the Doppler signal, is right such a kind of signal.

According to Equation 8 and Equation 11, we can calculate the 4π response to the Doppler signal by

$$d_{sidelobe} = \frac{T_0}{c} \mathbf{v} \cdot \sum_k \left[\frac{(G_k^A - G_k^B)}{N} \mathbf{n}_k \right], \quad (12)$$

where k stands for all sidelobe pixels.

Using ΔG^A and ΔG^B for the sidelobe gain uncertainties, and considering the fact that G^A and G^B are both constants in the spacecraft coordinate, we consequently obtain two constants in the spacecraft coordinate:

$$\Delta \mathbf{n}_A = \sum_k \frac{\Delta G_k^A \mathbf{n}_k}{N}, \quad \Delta \mathbf{n}_B = \sum_k \frac{\Delta G_k^B \mathbf{n}_k}{N}, \quad (13)$$

⁵ The transmission factors are omitted here, e.g., the ratio between the antenna temperature and CMB temperature, and the ratio between temperature and electronic digital unit. That means, with all these simplifications, if the antenna response is a δ function which is none zero only at the optical direction, then the recorded signal is simply $S = b$

⁶ Because the antennas are static in the spacecraft coordinate.

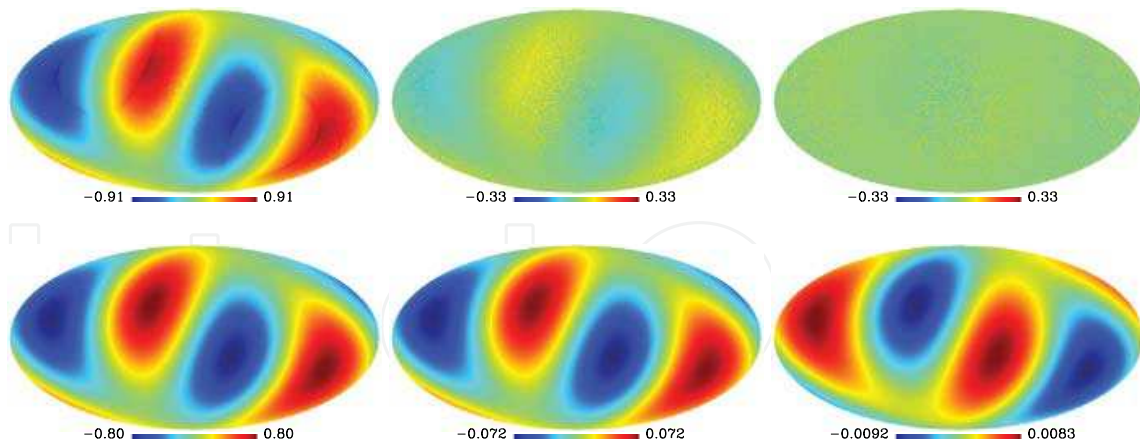


Fig. 11. *Top Panels:* The expected temperature deviation caused by the equivalent pointing vector error due to the sidelobe uncertainty issue in the WMAP mission. *Bottom panels:* The quadrupole components of the top panels. From left to right: The equivalent pointing vector error is along the x , y , z axes in the spacecraft coordinate respectively.

and the uncertainty of $d_{sidelobe}$ can be expressed as

$$\Delta d_{sidelobe} = \frac{T_0}{c} \mathbf{v} \cdot (\Delta \mathbf{n}_A - \Delta \mathbf{n}_B) = \frac{T_0}{c} \mathbf{v} \cdot \Delta \mathbf{n}. \quad (14)$$

$\Delta \mathbf{n}$ is called the equivalent pointing vector error, because it isn't a real pointing error, but has the same effect as real pointing vector errors caused by direct reasons or the timing issue.

It's apparent that we are interested in the gain uncertainty ΔG , not the gain itself. It's very difficult to accurately determine the antenna sidelobe response, at least due to three reasons: 1, the sidelobe response is very weak; 2, the signal due to the sidelobe response is always mixed with other much stronger signals (some are even unknown); 3, the sidelobe response of the two antennas could overlap and it's almost impossible to exactly solve for both. Therefore, it's not strange that the WMAP sidelobe gain has very high uncertainty: as presented by Barnes et al. (2003), up to 30%; however, the provides 30% uncertainty contains only the average level uncertainty, with no inclusion of the pixel-to-pixel variance. Thus the overall uncertainty must be much higher than the claimed 30%.

It's well known that the dot product of two vectors is invariant in coordinate transform, thus we can calculate $\Delta d_{sidelobe}$ in any coordinates using Equation 14, and the result will be the same. Since $\Delta \mathbf{n}$ is determined by the gain and antenna pointing vectors, which are both constants in the spacecraft coordinate, the best coordinate to calculate $\Delta d_{sidelobe}$ is certainly the spacecraft coordinate. However, even in the spacecraft coordinate, it's still impossible to exactly calculate the uncertainty due to $\Delta \mathbf{n}$ (otherwise it won't be called the "uncertainty"). In this case, a possible way out is to divide $\Delta \mathbf{n}$ into three components Δn_x , Δn_y , Δn_z along the X , Y , Z axes of the spacecraft coordinate. For each component, we can set any amplitude for it (we will explain why we can do like this below) and use the corresponding $\Delta d_{sidelobe}$ instead of the differential data to obtain an output map ΔT_x , ΔT_y or ΔT_z like we did for the real TOD in Sec. 2.1. Examples of ΔT_x , ΔT_y , ΔT_z are presented in Fig. 11.

Both Fig. 10 and Fig. 11 illustrate the same thing: there could be significant systematical error in the WMAP CMB detection. Fig. 11 tell us more, that even if the antenna pointing vectors

are accurate, it's still impossible to conclude that the CMB results are hence reliable. Not to mention the fact confirmed by Roukema (2010b) and Liu, Xiong & Li (2011) that there are more potential uncertainties in the data calibration. Thus it's really too early to be so sure about the CMB detection or a final CMB model right now.

4.6 How to remove the artificial components?

We have seen possible CMB temperature deviations due to real or equivalent antenna pointing errors in Fig 10, 11, but they don't 100% ensure that the final CMB result by WMAP is wrong. However, we can still do something to get a more reasonable CMB estimation. We know that if there is extra uncertainty due to any reason in CMB detection, the corresponding deviation map, if available, should be removed from the final CMB temperature map to ensure a clean and reliable result. Now we have successfully obtained the final temperature deviation pattern due to the possible pointing error (Fig. 10 or Fig. 11, no matter real or equivalent), then we surely need to remove it from the obtained CMB results. The last hamper is that we don't know the exact amplitude of Δn_x , Δn_y , Δn_z ; however, there are already methods for that, which has already been adopted by the WMAP team in removing the foreground emission.

When we try to remove the foreground emission, we are facing exactly the same difficulty: The foreground emission can be modeled by astrophysical emission mechanism including free-free, synchrotron, and dust emissions, however, the exact amplitude of each emission mechanism can't be predicted by the model. Moreover, all emission mechanism take effect together in CMB detection, and they are also combined with the CMB signal, thus the only way to determine the amplitudes of each emission mechanism is by model fitting. In this process, three a priori emission maps are presented as T_{ff} , T_{sync} , and T_{dust} (Bennett et al., 2003; Finkbeiner et al., 1999; Finkbeiner, 2003; Gold et al., 2009), and the clean temperature T is supposed to be

$$T = T^* - c_{ff}T_{ff} - c_{sync}T_{sync} - c_{dust}T_{dust}, \quad (15)$$

where the amplitudes c_{ff} , c_{sync} , c_{dust} are calculated by least-square fitting. The same technic can be used here: The real CMB temperature should be

$$T = T^* - c_x\Delta T_x - c_y\Delta T_y - c_z\Delta T_z, \quad (16)$$

and like above, the coefficients c_x , c_y , c_z can be determined by least-square fitting. It's important to notice that, in least square fitting, the amplitudes of the templates ΔT_x , ΔT_y , ΔT_z are not important, that's why we said above that we can use any amplitude for Δn_x , Δn_y , and Δn_z . As shown by Liu & Li (2010), the result is well consistent to our previous work (Liu & Li, 2009b): the CMB quadrupole after template fitting removal is about $10 \sim 20 \mu\text{K}$, much lower than the WMAP release. In other words, without supposing an a priori pointing error, we have self-consistently confirmed it posteriorly.

5. Planck and future CMB detection missions

Although the Planck spacecraft is significantly improved compared to WMAP, the basic detecting method are similar: antenna that suffers from 4π sidelobe response is used; the spacecraft works on the same L2 spot; the scan pattern is similar: a three-axis rotation consists of rotation around the Sun, spin around it's symmetry axis, and cycloidal procession around the Sun-to-spacecraft axis. Thus the three factors we have listed: direct pointing error, timing error, and sidelobe uncertainty can all take effect in the Planck mission. We have simulated the

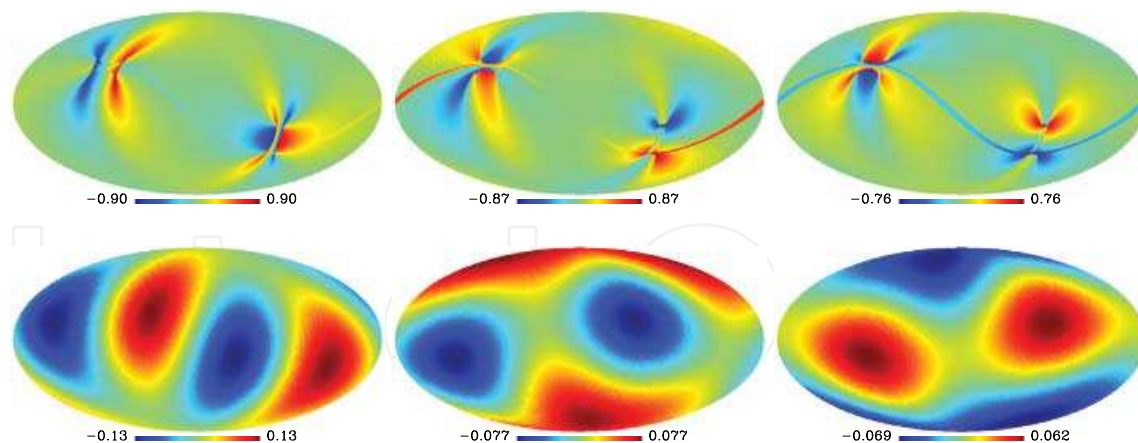


Fig. 12. *Top Panels:* The expected temperature deviation caused by the equivalent pointing vector error due to the sidelobe uncertainty issue in the Planck mission. *Bottom panels:* The quadrupole components of the top panels. From left to right: The equivalent pointing vector error is along the x , y , z axes in the spacecraft coordinate respectively.

Planck scan strategy and possible resulting CMB deviation due to real or equivalent pointing vector error (Liu & Li, 2011), and found that similar CMB deviation may also occur in the Planck mission, as shown in Fig. 12. If in the final data release of Planck, the CMB result after least-square fitting removal is consistent to the WMAP result with the similar treatment, then the corresponding result would certainly be more robust and import.

6. Discussion

Understanding systematic effects in experiments and observations is a difficult task. It is not strange for a newly explored waveband in astronomy that early observation results contain unaware systematics. As an example, COS B is the second mission for gamma-ray band. The COS B group published the 2CG catalog of high energy gamma-ray sources detected with the selection criteria for no more than one spurious detection above the adopted threshold from background fluctuation could be expected (Swanenburg et al., 1981). However, Li & Wolfendale (1982) found that about half of the released 25 sources are pseudo-ones produced by Galactic gamma-ray background fluctuation. The mistake came from a simplified model of the diffuse Galactic gamma-rays used by the COS B group, leading to systematically overestimate significance of source detection. After many years debating, the pseudo-sources have been finally deleted from the 2CG catalog, and instead of the simplified background model, more reliable structured models for diffuse Galactic gamma-rays have been adopted by all following gamma-ray missions. For microwave band, WMAP is just the second mission. Although the WMAP team made huge effort to study systematic effects, there still notably exist systematic errors in their released results. It seems that the foreground issue has been carefully and effectively treated, but the CMB dipole effect has not yet. The Doppler-dipole moment dominates CMB anisotropies, various errors in CMB experiments can produce pseudo-dipole signals and then artificial anisotropies in resultant CMB maps, seriously affecting cosmological studies. Beside the foreground emissions, the pseudo-dipole-induced anisotropy is another key systematic problem common for all CMB missions. Without carefully and effectively treating the dipole issue, CMB maps from COBE, WMAP, and Planck are not reliable for studying the CMB anisotropy.

However, we still have to notice one thing: we have confirmed that the early discovered anomalies (Sec. 1) still exist after least-square fitting removal, although they do seem to be weakened. Another fact also need to be noticed: Both the WMAP CMB quadrupole and octupole is aligned with the Ecliptic plane and each other (Bielewicz et al., 2004; Copi et al., 2004), however, after least-square fitting removal, the quadrupole no longer aligned with either one, but the octupole still aligned with the Ecliptic plane. This two facts may indicate that there are still unresolved problems in the WMAP mission!

7. Acknowledgments

This work is Supported by the National Natural Science Foundation of China (Grant No. 11033003). The data analysis made use of the WMAP data archive and the HEALPix software package.

8. References

- Barnes C., et al. (2003). First-Year Wilkinson Microwave Anisotropy Probe (WMAP) Observations: Galactic Signal Contamination from Sidelobe Pickup, *The Astrophysical Journal Supplement Series*, 148, 51-62
- Bennett C. L., et al. (2003). First-Year Wilkinson Microwave Anisotropy Probe (WMAP) Observations: Preliminary Maps and Basic Results, *The Astrophysical Journal Supplement Series*, 148, 1-27
- Bielewicz P., Górski K. M., Banday A. J. (2004). Low-order multipole maps of cosmic microwave background anisotropy derived from WMAP, *Monthly Notices of the Royal Astronomical Society*, 355, 1283-1302
- Copi C. J., Huterer D., Starkman G. D. (2004). Multipole vectors: A new representation of the CMB sky and evidence for statistical anisotropy or non-Gaussianity at $2 \leq l \leq 8$, *Physical Review D*, 70, 043515-
- Copi C. J., Huterer D., Schwarz D. J., Starkman G. D. (2007). Uncorrelated universe: Statistical anisotropy and the vanishing angular correlation function in WMAP years 1-3, *Physical Review D*, 75, 023507-
- Cruz M., Martínez-González E., Vielva P., Cayón L. (2005). Detection of a non-Gaussian spot in WMAP, *Monthly Notices of the Royal Astronomical Society*, 356, 29-40
- Cruz M., Cayón L., Martínez-González E., Vielva P., Jin J. (2007). The Non-Gaussian Cold Spot in the 3 Year Wilkinson Microwave Anisotropy Probe Data, *The Astrophysical Journal*, 655, 11-20
- Eriksen H. K., Banday A. J., Górski K. M., Lilje P. B. (2005). The N-Point Correlation Functions of the First-Year Wilkinson Microwave Anisotropy Probe Sky Maps, *The Astrophysical Journal*, 622, 58-71
- Eriksen H. K., Banday A. J., Górski K. M., Hansen F. K., Lilje P. B. (2007). Hemispherical Power Asymmetry in the Third-Year Wilkinson Microwave Anisotropy Probe Sky Maps, *The Astrophysical Journal*, 660, L81-L84
- Finkbeiner D. P., Davis M., Schlegel D. J. (1999). Extrapolation of Galactic Dust Emission at 100 Microns to Cosmic Microwave Background Radiation Frequencies Using FIRAS, *The Astrophysical Journal*, 524, 867-886
- Finkbeiner D. P. (2003). A Full-Sky $H\alpha$ Template for Microwave Foreground Prediction, *The Astrophysical Journal Supplement Series*, 146, 407-415

- Gold B., et al. (2009). Five-Year Wilkinson Microwave Anisotropy Probe Observations: Galactic Foreground Emission, *The Astrophysical Journal Supplement Series*, 180, 265-282
- Hansen F. K., Cabella P., Marinucci D., Vittorio N. (2004). Asymmetries in the Local Curvature of the Wilkinson Microwave Anisotropy Probe Data, *The Astrophysical Journal*, 607, L67-L70
- Hansen F. K., Banday A. J., Eriksen H. K., Górski K. M., Lilje P. B. (2006). Foreground Subtraction of Cosmic Microwave Background Maps Using WI-FIT (Wavelet-Based High-Resolution Fitting of Internal Templates), *The Astrophysical Journal*, 648, 784-796
- Hinshaw G., et al. (2003). First-Year Wilkinson Microwave Anisotropy Probe (WMAP) Observations: Data Processing Methods and Systematic Error Limits, *The Astrophysical Journal Supplement Series*, 148, 63-95
- Hinshaw G., et al. (2003). First-Year Wilkinson Microwave Anisotropy Probe (WMAP) Observations: The Angular Power Spectrum, *The Astrophysical Journal Supplement Series*, 148, 135-159
- Komatsu E., et al. (2003). First-Year Wilkinson Microwave Anisotropy Probe (WMAP) Observations: Tests of Gaussianity, *The Astrophysical Journal Supplement Series*, 148, 119-134
- Li T.P., Wolfendale A.W. (1982). Discret sources of cosmic gamma rays, *Astronomy and Astrophysics*, 116, 95-100
- Li T.P., Liu H., Song L.-M., Xiong S.-L., Nie J.-Y. (2009). Observation number correlation in WMAP data, *Monthly Notices of the Royal Astronomical Society*, 398, 47-52
- Liu H., Li T.P. (2009). Systematic distortion in cosmic microwave background maps, *Science in China G: Physics and Astronomy*, 52, 804-808
- Liu H., Li T.P. (2009). Improved CMB Map from WMAP Data, *ArXiv e-prints*, arXiv:0907.2731
- Liu H., Xiong S.L., Li T.P. (2010). The origin of the WMAP quadrupole, *ArXiv e-prints*, arXiv:1003.1073
- Liu H., Li T. P. (2010). Pseudo-Dipole Signal Removal from WMAP Data, *Chinese Science Bulletin*, 56(1) 29-33
- Liu H., Xiong S.L., Li T.P. (2011). Diagnosing timing error in WMAP data, *Monthly Notices of the Royal Astronomical Society*, 413, L96-L100
- Liu H., Li T.P. (2011). Observational Scan-Induced Artificial Cosmic Microwave Background Anisotropy, *The Astrophysical Journal*, 732, 125
- Liu X., Zhang S. N. (2005). Non-Gaussianity Due to Possible Residual Foreground Signals in Wilkinson Microwave Anisotropy Probe First-Year Data Using Spherical Wavelet Approaches, *The Astrophysical Journal*, 633, 542-551
- McEwen J. D., Hobson M. P., Lasenby A. N., Mortlock D. J. (2006). A high-significance detection of non-Gaussianity in the WMAP 3-yr data using directional spherical wavelets, *Monthly Notices of the Royal Astronomical Society*, 371, L50-L54
- Moss A., Scott D., Zibin J. P. (2010). No evidence for anomalously low variance circles on the sky, *ArXiv e-prints*, arXiv:1012.1305
- Roukema B. F. (2010). On the suspected timing error in Wilkinson microwave anisotropy probe map-making, *Astronomy and Astrophysics*, 518, A34
- Roukema B. F. (2010). On the suspected timing-offset-induced calibration error in the Wilkinson microwave anisotropy probe time-ordered data, *ArXiv e-prints*, arXiv:1007.5307
- Sawangwit, U. & Shanks, T. (2010). Is everything we know about the universe wrong? *Astronomy & Geophysics*, 51: 5.14C5.16

- Swanenburg B.N. et al., (1981). Second COS B catalog of high energy gamma-ray sources, *The Astrophysical Journal*, 243, L69
- Vielva P., Martínez-González E., Barreiro R. B., Sanz J. L., Cayn L. (2004). Detection of Non-Gaussianity in the Wilkinson Microwave Anisotropy Probe First-Year Data Using Spherical Wavelets, *The Astrophysical Journal*, 609, 22-34
- Vielva P., Wiaux Y., Martínez-González E., Vandergheynst P. (2007). Alignment and signed-intensity anomalies in Wilkinson Microwave Anisotropy Probe data, *Monthly Notices of the Royal Astronomical Society*, 381, 932-942
- Wiaux Y., Vielva P., Martínez-González E., Vandergheynst P. (2006). Global Universe Anisotropy Probed by the Alignment of Structures in the Cosmic Microwave Background, *Physical Review Letters*, 96, 151303-

IntechOpen



Space Science

Edited by Dr. Herman J. Mosquera Cuesta

ISBN 978-953-51-0423-0

Hard cover, 152 pages

Publisher InTech

Published online 23, March, 2012

Published in print edition March, 2012

The all-encompassing term Space Science was coined to describe all of the various fields of research in science: Physics and astronomy, aerospace engineering and spacecraft technologies, advanced computing and radio communication systems, that are concerned with the study of the Universe, and generally means either excluding the Earth or outside of the Earth's atmosphere. This special volume on Space Science was built throughout a scientifically rigorous selection process of each contributed chapter. Its structure drives the reader into a fascinating journey starting from the surface of our planet to reach a boundary where something lurks at the edge of the observable, light-emitting Universe, presenting four Sections running over a timely review on space exploration and the role being played by newcomer nations, an overview on Earth's early evolution during its long ancient ice age, a reanalysis of some aspects of satellites and planetary dynamics, to end up with intriguing discussions on recent advances in physics of cosmic microwave background radiation and cosmology.

How to reference

In order to correctly reference this scholarly work, feel free to copy and paste the following:

Hao Liu and Ti-Pei Li (2012). Systematics in WMAP and Other CMB Missions, Space Science, Dr. Herman J. Mosquera Cuesta (Ed.), ISBN: 978-953-51-0423-0, InTech, Available from:

<http://www.intechopen.com/books/space-science/systematics-in-wmap-and-other-cmb-missions>

INTECH
open science | open minds

InTech Europe

University Campus STeP Ri
Slavka Krautzeka 83/A
51000 Rijeka, Croatia
Phone: +385 (51) 770 447
Fax: +385 (51) 686 166
www.intechopen.com

InTech China

Unit 405, Office Block, Hotel Equatorial Shanghai
No.65, Yan An Road (West), Shanghai, 200040, China
中国上海市延安西路65号上海国际贵都大饭店办公楼405单元
Phone: +86-21-62489820
Fax: +86-21-62489821

© 2012 The Author(s). Licensee IntechOpen. This is an open access article distributed under the terms of the [Creative Commons Attribution 3.0 License](#), which permits unrestricted use, distribution, and reproduction in any medium, provided the original work is properly cited.

IntechOpen

IntechOpen